Streaming Instability in Growing Cell Populations

William Mather[1], **Octavio Mondragón-Palomino**[1], **Tal Danino**[1], **Jeff Hasty**[2,1,3], and **Lev S. Tsimring**[3,*]

[1]Department of Bioengineering, UCSD, 9500 Gilman Dr., La Jolla, California 92093-0412, USA

[2]Molecular Biology Section, Division of Biology, UCSD, 9500 Gilman Dr., La Jolla, California 92093-0368, USA

[3]BioCircuits Institute, UCSD, 9500 Gilman Dr., La Jolla, California 92093-0328, USA

Abstract

Flows of cells growing as a quasimonolayer in a confined space can exhibit streaming, with narrow streams of fast-moving cells flowing around clusters of slowly moving cells. We observed and analyzed this phenomenon experimentally for *E. coli* bacteria proliferating in a microfluidic cell trap using time-lapse microscopy. We also performed continuum modeling and discrete-element simulations to elucidate the mechanism behind the streaming instability. Our analysis demonstrates that streaming can be explained by the interplay between the slow adaptation of a cell to its local microenvironment and its mobility due to changes of cell-substrate contact forces.

Microorganisms employ a wide range of cooperative strategies for responding to adverse environmental conditions [1–5]. In many cases, these strategies lead to intricate patterns and complex shapes in bacterial colonies [6–8]. While such patterning is usually associated with long-range cell signaling and motility [9], microorganisms are often found in dense communities where direct cellular contact plays an important role in the dynamics of colony formation [10,11]. Moreover, bacteria often actively seek to aggregate in small cavities and crevices, which helps them to cope with environmental conditions [12,13]. In our recent work [14] we studied orientational ordering of bacteria caused by their growth and ensuing hydrodynamic flow. Here, we use microfluidic traps to characterize a general streaming instability occurring in a confined colony of nonmotile bacteria. In order to investigate the mechanism driving the streaming instability, we develop a continuum model and complementary discrete-element simulations with cells modeled as growing and dividing soft spherocylinders which adapt their size and mobility to local microenvironments.

In order to study bacterial colony growth in a confined environment, we constructed microfluidic devices featuring two types of traps (open and side) capable of sustaining a two-dimensional colony of nonmotile bacteria *E. coli* over many generations. Open traps are ~1 μm-deep rectangular regions of different horizontal dimensions (up to $200 \times 2000\ \mu m^2$) embedded in the middle of the 6–10 μm-deep main channel [see Fig. 1(a)]. The external fluid flow through the main channel (~50 μm/ sec) delivers nutrients to the open boundaries of the trap, allowing for their diffusion into the interior of the trap. The fluid flow in the channel also removes metabolic waste and cells ejected from the trap. Side traps have similar dimensions but are embedded in the side walls of the main channel and have only one open boundary [Fig. 1(b)].

*ltsimring@ucsd.edu .

In the beginning of each experiment we placed a few bacteria inside the trap and waited several hours (mean cell division time was about 20 min) until the colony grew and filled the trap region completely. The subsequent growth was balanced by a significant expansion flow towards the open boundaries of the trap. We found that the expansion flow of growing cells inside the traps was surprisingly nonuniform. This behavior was quantitatively analyzed by particle image velocimetry software MATPIV [15]. Figure 1(c) illustrates that cells escape from an open trap into the main channel in narrow rapidly moving *streams* that bypass regions of almost stagnant cells localized near the open boundaries (see also movie S1 [16]). The cell streams are dynamic [see Fig. 1(d)]; the number and positions of streams fluctuate over the duration of a typical experiment. Similar results were obtained in side-trap experiments; see [16]. More detailed inspection of the cells inside the traps revealed that stagnant cells are generally thicker than rapidly moving cells comprising the streams. Furthermore, the cell size is strongly dependent on its distance from the open boundary of the trap: in the trap interior the cell diameter is only half of that near the open boundaries (where the diameter is about 1 μm) [16]. There may be multiple factors which can cause this dependence, from nutrient depletion to waste accumulation and quorum signaling. Our estimate [16] gives the characteristic preferred carbon source depletion distance of the order of 25 μm from the open boundary, which is consistent with the observed transition to smaller cell sizes.

The instability in cellular streams can be understood in terms of the interplay between the cell size and its mechanical properties. Since the trap height is nearly equal to the cell diameter, the mechanical interaction between the cells and the top and bottom walls of the trap affects their mobility. Under the same pressure gradient, smaller cells experience less drag and move faster, while larger cells experience higher drag and move slower. As cells move towards the open boundary, they grow larger in diameter, which leads to their reduced mobility. The streaming instability occurs when the growth rate of the diameter is comparable to the time a cell spends moving from the back of the trap to the open boundary. Under this condition, slowly moving cells grow larger and can effectively stop moving and form obstacles that permit streaming patterns to emerge for smaller, fast-moving cells.

We developed a continuum model of the colony dynamics which generalizes equations of two-dimensional incompressible fluid dynamics to include the effects of cell growth and drag force, the latter arising from the interaction of the cells with the floor and ceiling of the trap. We did not include the effects of cell shape and position-dependent growth rate in the model since they do not appear to be essential for the basic streaming mechanism. The incompressible "cell fluid" of constant density (scaled to 1) is described by the following equations $\left(D/Dt \equiv \partial/\partial t + \vec{v} \cdot \vec{\nabla} \right)$:

$$\frac{D\vec{v}}{Dt} = -\vec{\nabla} p - g\left(f\right)\vec{v} + \mu\nabla^2\vec{v} \tag{1}$$

$$\frac{Df}{Dt} = \gamma\left(c\left(\vec{r}\right) - f\right) \tag{2}$$

$$\vec{\nabla} \cdot \vec{v} = \alpha \tag{3}$$

with $\vec{v}$ the cell velocity field, p the pressure field, f a field characterizing cell diameter, $g(f)$ an f-dependent coefficient of (top and bottom) drag for cells moving in the shallow trap, γ the rate

of f adaptation to the local chemical environment, μ a coefficient of effective viscosity for cell flow, and α the volumetric growth rate of the "cell fluid." According to Eq. (2), cell "diameter" f of a cell at a fixed position $\vec{r}$ reaches an equilibrium value $c\left(\vec{r}\right)$ that is chosen to be highest near an open boundary of the cell trap. Thus, stagnant cells become largest near the trap opening. The somewhat unusual form of the incompressibility equation (3) is due to the presence of a distributed mass source due to exponential cell growth. This equation can be used to find the hydrodynamic pressure p. We impose the boundary condition of a constant pressure at the open sides of the trap. The drag coefficient $g(f)$ is assumed to nonlinearly increase with f, due to the appearance of strong contact friction between the cell and the trap for large cells. In all results given below we have used $g(f) = f^2$, although the specific form of the nonlinearity is not essential. We also neglect cell inertia and employ the over-damped limit for the momentum equation $\left(D\vec{v}/Dt \approx 0\right)$.

The analysis simplifies considerably in the case of narrow-channel flow (small x dimension), where Eqs. (1)–(3) in the overdamped limit can be reduced to the one-dimensional system

$$\frac{\partial p}{\partial z} = -g(f)v + \mu\frac{\partial^2 v}{\partial z^2},$$

(4)

$$\frac{\partial f}{\partial t} + v\frac{\partial f}{\partial z} = \gamma(c(z) - f),$$

(5)

$$\frac{\partial v}{\partial z} = \alpha.$$

(6)

Equation (6) stipulates a linear velocity profile $v(z, t) = \alpha z + v_0(t)$. In a side trap with the solid wall at $z = 0$ and the open boundary at $z = L_z$, $v_0(t) = 0$, and the velocity, pressure, and f fields are asymptotically stationary and unique. The open-trap case (open boundaries at $z = \pm L_z$) is more interesting, since $v_0(t)$ can be a function of time. Substituting the expression for $v(z, t)$ in Eq. (4) and integrating the latter from $-L_Z$ to L_z with the boundary condition $p(L_z) = p(-L_z)$ we obtain $v_0(t) = -\alpha G_1[f]/G_0[f]$, where $G_s[f] = \int_{-L_z}^{L_z} dz z^s g(f(z,t))$. This formula defines the flow velocity for a known field $f(z, t)$. The remaining Eq. (5) can be solved through a polynomial mode expansion $f(z,t) = \sum_{n=0}^{\infty} f_n(t)z^n$, $c(z) = \sum_{n=0}^{\infty} c_n z^n$ and truncation to a finite-dimensional set of nonlinear ODEs (see [16] for the straightforward derivation). The numerical bifurcation analysis of the system using MATCONT [17] reveals that the narrow-channel flow in an open trap exhibits a variety of dynamic regimes, including symmetric flow ($v_0 = 0$), asymmetric flow ($v_0 = \text{const} \neq 0$), and oscillatory flow [$v_0(t)$ is periodic], depending on parameters; see Fig. 2(a) and 2(b). We indeed observed nonstationary asymmetric flow regimes in discrete-element simulations and the open-trap experiments [16]. It is also interesting to note the possibility of bistable regimes (e.g., bistability between oscillations and uniform flow).

The onset of cell streaming in the full two-dimensional model can be determined by the linear stability analysis of the transversally uniform flow with respect to small periodic in x perturbations. We consider here the case of the stationary zero-order solution, $v^{(0)}(z)$, $p^{(0)}(z)$ and $f^{(0)}(z)$. In the first order, these solutions are perturbed by the functions $\{\tilde{v}_z, \tilde{v}_x; \tilde{p}, \tilde{f}\} = \{V(z), iV'(z)/k, P(z), F(z)\} \times \exp(ikx + \lambda t)$ (the velocity components $\tilde{v}_x$, $\tilde{v}_z$ satisfy incompressibility

condition automatically). Substituting this ansatz in Eqs. (1)–(3) we arrive at a 1D eigenvalue problem for λ, $V(z)$, $P(z)$, and $F(z)$ with corresponding boundary conditions for side or open-trap cases. In case of the side trap, the boundary conditions are $V(0) = F(0) = P(L_z) = 0$, and for a symmetric flow in an open trap, the b.c. are $P(\pm L_z) = F(0) = 0$. Additionally, we assume a continuous tangential stress condition (slip) at both the inner wall and the outer free boundary, $k^2 V(z) + V''(z) = 0$, $z = 0$, L. This problem can be solved numerically by a shooting-matching method. The streaming instability first occurs near the wave number $k \approx 2L_z^{-1}$; see Figs. 2(c) and 2(d). This instability requires the presence of a sufficiently steep gradient in the friction field $g(f)$. Intermediate values for the relaxation rate (i.e. $\gamma \approx \alpha$) also are required for the instability, such that adaptation to the chemical microenvironment occurs on a time scale comparable to cell division time. Finally, the streaming instability was found to be sensitive to the value of the coefficient of viscosity μ [Fig. 2(c)].

The two-dimensional continuum analysis of streaming addressed only the linear stability of uniform flow. In addition, the continuum model does not include granular effects, including cell shape [18]. We therefore performed discrete-element simulations (DES) of growing and dividing rodlike cells in a two-dimensional monolayer using a generalization of the soft-particle algorithm described in Ref. [14]. We introduced an internal variable f carried with each "cell" and inherited by its offspring. The variable f for each cell obeys the equation

$df/dt = \gamma\left(c\left(\vec{r}\right) - f\right)$ analogous to Eq. (2). Cells grow at a rate proportional to their length and divide on average at the length ℓ_{div}. Escape of cells from the trap is treated by removing cells when their centers cross the open boundary of the trap.

Simulations for cells in a side-trap geometry provide an extension of the linear stability analysis presented above. In the parameter region corresponding to the linear instability we have found significant streaming (see Fig. 3 and [16] movies S6 and S7). Similar to experiment, the structures in simulations remain dynamic, allowing drifting, merging, and spontaneous creation of streams. Since in most simulations traps of moderate horizontal dimensions (up to 150 cell diameters) were explored, as expected, the granular effects played a significant role in stabilizing streaming instability for cells with relatively small aspect ratios (e.g., $\ell_{div}=3$). In particular, we found that the system could be bistable between uniform flow and streaming pattern [see Fig. 3(b) and 3(c)]. These results demonstrate that the linear instability of uniform flow gives only a sufficient condition for streaming.

We also probed the effects of cell orientation on cell streaming by analyzing different cell aspect ratios. Longer cells within the streams tend to align their axis along the flow as expected [14]. This enhanced ordering locally reduces effective shear viscosity, since aligned long cells easily slide past each other (cell-cell friction is assumed small), and this further increases the intensity of streaming [see Fig. 3(d) and [16] movie S7 for $\ell_{div}=5$].

Our theoretical and numerical results indicate that the streaming instability arises due to the strong dependence of cell mobility on its size due to drag from top and bottom of the trap. This implies that the streaming instability should be sensitive to the depth of the trap. Additional experiments in deeper traps (1.65 μm) indeed demonstrated the loss of cell streaming [16].

In summary, we have shown that flows of bacteria growing in confined spaces are prone to a streaming instability. The mechanism of the streaming instability is related to the coupling between the cell growth and mobility: larger cells experience greater drag force when moving within a confined space. Cell size, in turn, depends on local chemical environment. In our experiments, cells grow larger near the edge of the trap where the nutrient concentration is higher and waste concentration is lower. The longer the cell remains near the edge of the trap, the larger it becomes and the more difficult it becomes for it to leave the trap. Smaller cells, which are growing in the bulk of the colony, are forced to bypass the larger static cells and

form narrow streams. These streams are reminiscent of Saffman-Taylor viscous fingers at an interface between two fluids with different viscosities [19,20]. While we observed the streaming instability in laboratory strains of bacteria grown in microfluidic environments, we believe that the phenomenon is fairly generic and is likely to occur in dense colonies in natural habitats, since bacteria often are found in dense populations in small cavities and crevices where they from biofilms. Future investigations of streaming in biofilms may benefit from the inclusion of effects not included in the present investigation, such as cell-cell and cell-trap adhesion due to an extracellular polymeric matrix. More generally, the interplay between physical properties of cells and their mobility may play an important role in other examples of morphogenesis, such as invasive tumor growth [21].

Supplementary Material

Refer to Web version on PubMed Central for supplementary material.

Acknowledgments

References

1. Shapiro JA. Annu. Rev. Microbiol 1998;52:81. [PubMed: 9891794]

2. Bassler BL. Cell 2002;109:421. [PubMed: 12086599]

3. Stoodley P, Sauer K, Davies DG, Costerton JW. Annu. Rev. Microbiol 2002;56:187. [PubMed: 12142477]

4. Donlan RM. Emerging Infectious Diseases 2002;8:881. [PubMed: 12194761]

5. Stewart PS, Franklin MJ. Nat. Rev. Microbiol 2008;6:199. [PubMed: 18264116]

6. Ben-Jacob E, Cohen I, Shochet O, Aranson I, Levine H, Tsimring LS. Nature (London) 1995;373:566. [PubMed: 7854411]

7. Levine H, Aranson I, Tsimring L, Truong TV. Proc. Natl. Acad. Sci. U.S.A 1996;93:6382. [PubMed: 8692824]

8. Dockery J, Klapper I. SIAM J. Appl. Math 2002;62:853.

9. Park S, Wolanin PM, Yuzbashyan EA, Lin H, Darnton NC, Stock JB, Silberzan P, Austin R. Proc. Natl. Acad. Sci. U.S.A 2003;100:13 910.

10. Tolker-Nielsen T, Brinch UC, Ragas PC, Andersen JB, Jacobsen CS, Molin S. J. Bacteriol 2000;182:6482. [PubMed: 11053394]

11. Drasdo D. Phys. Rev. Lett 2000;84:4244. [PubMed: 10990656]

12. Shimp R, Pfaender F. Appl. Environ. Microbiol 1982;44:471. [PubMed: 16346080]

13. Monier J, Lindow S. Proc. Natl. Acad. Sci. U.S.A 2003;100:15 977. [PubMed: 12509513]

14. Volfson D, Cookson S, Hasty J, Tsimring LS. Proc. Natl. Acad. Sci. U.S.A 2008;105:15 346.

15. Sveen, JK. An Introduction to MatPIV v.1.6.1. Dept. of Mathematics, University of Oslo; Oslo: 2004. http://www.math.uio.no/~jks/matpiv

16. See supplementary material at http://link.aps.org/supplemental/10.1103/PhysRevLett.104.208101

17. Dhooge A, Govaerts W, Kuznetsov YA. ACM Trans. Math. Softw 2003;29:141.

18. Jaeger HM, Nagel SR, Behringer RP. Rev. Mod. Phys 1996;68:1259.

19. Casademunt J, Magdaleno FX. Phys. Rep 2000;337:1.

20. Bensimon D, Kadanoff LP, Liang SD, Shraiman BI, Tang C. Rev. Mod. Phys 1986;58:977.

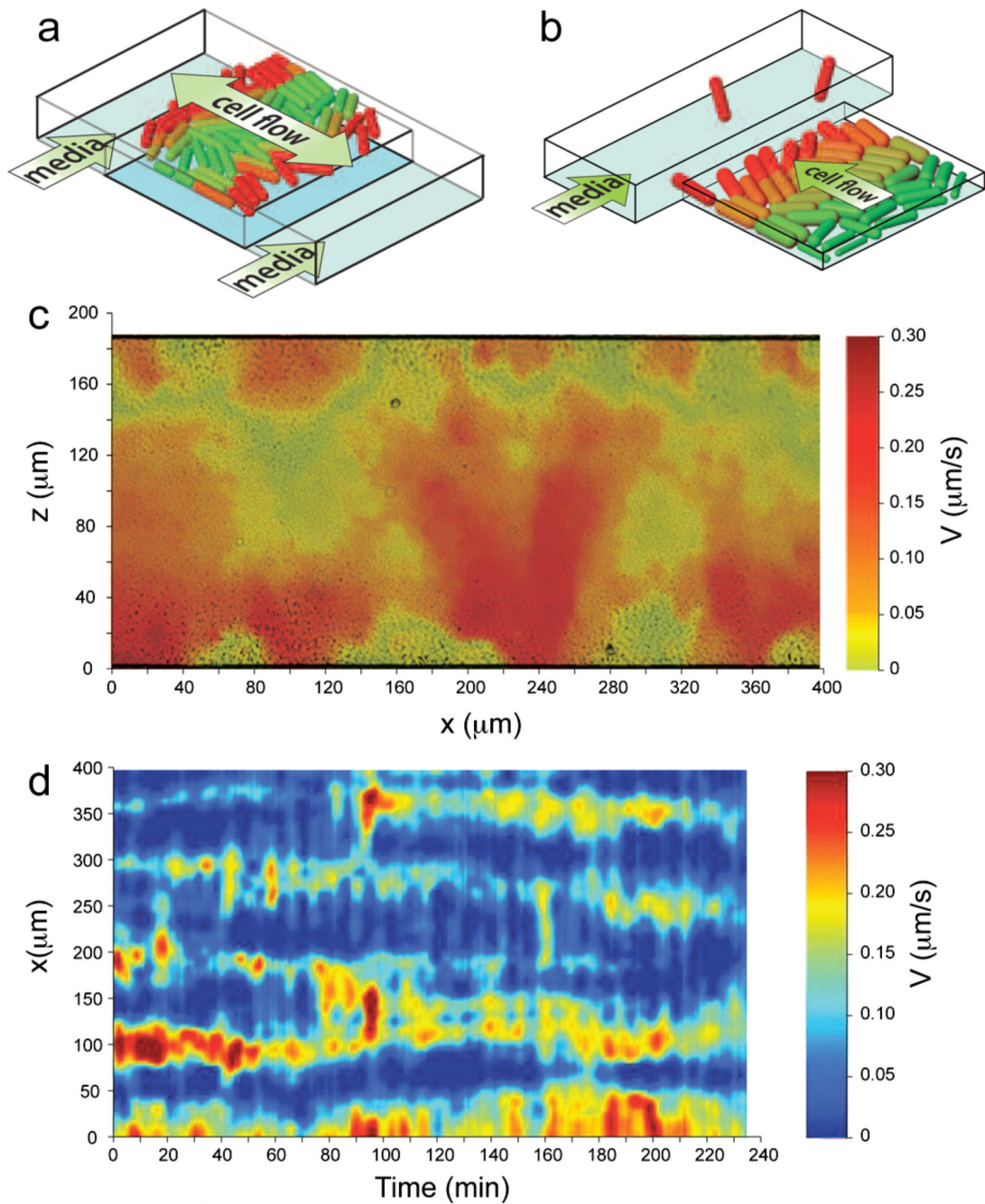21. Anderson ARA, Quaranta V. Nat. Rev. Cancer 2008;8:227. [PubMed: 18273038]

FIG. 1.
(color online). (a),(b) Schematic views of the microfluidic devices with open and side traps.
(c) Magnitude of the vertical component of cell velocity overlaid on a phase contrast image of
the trap at time 210 min of the run shown in movie S1; (d) Space-time plot of the cells' exit
velocity component averaged over the lower 20 μm of the trap in (c).
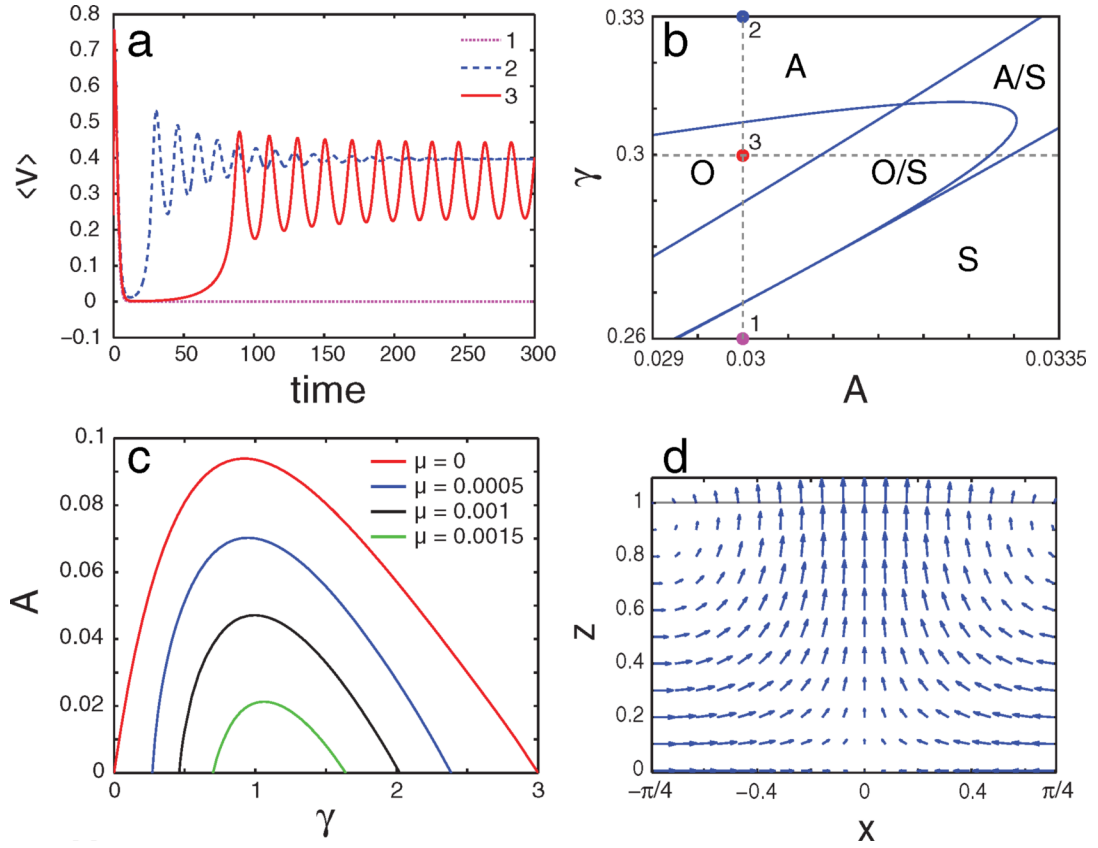
FIG. 2.

(color online). Results of the continuum hydrodynamic model in the overdamped limit using $c(z) = A + (z/L_z)^2$, $L_z = 1$, $\alpha = 1$. (a) Three regimes of narrow-channel flows: symmetric (1), asymmetric (2), and periodic (3) flows; (b) Bifurcation diagram of the narrow-channel flows in the (A, γ) plane. Symbol S denotes symmetric flow, A, asymmetric, and O, oscillatory flow regimes, double symbols (A/S, O/S) indicate domains of bistability according to local bifurcation analysis. Points 1,2,3 correspond to time series shown in (a). (c) Streaming instability domain in the parameter plane (A, γ) for different values of viscosity coefficient μ. Streaming for a given μ occurs for A below the corresponding curve; (d) Velocity field for the eigenfunction near the onset of a streaming instability, with wave vector $k = 2$, $\gamma = 1$, $A = 0.045$, $\mu = 0.001$. Since the flow is inverted for $\pi/4 \leq x \leq 3\pi/4$, only half the x period is displayed.
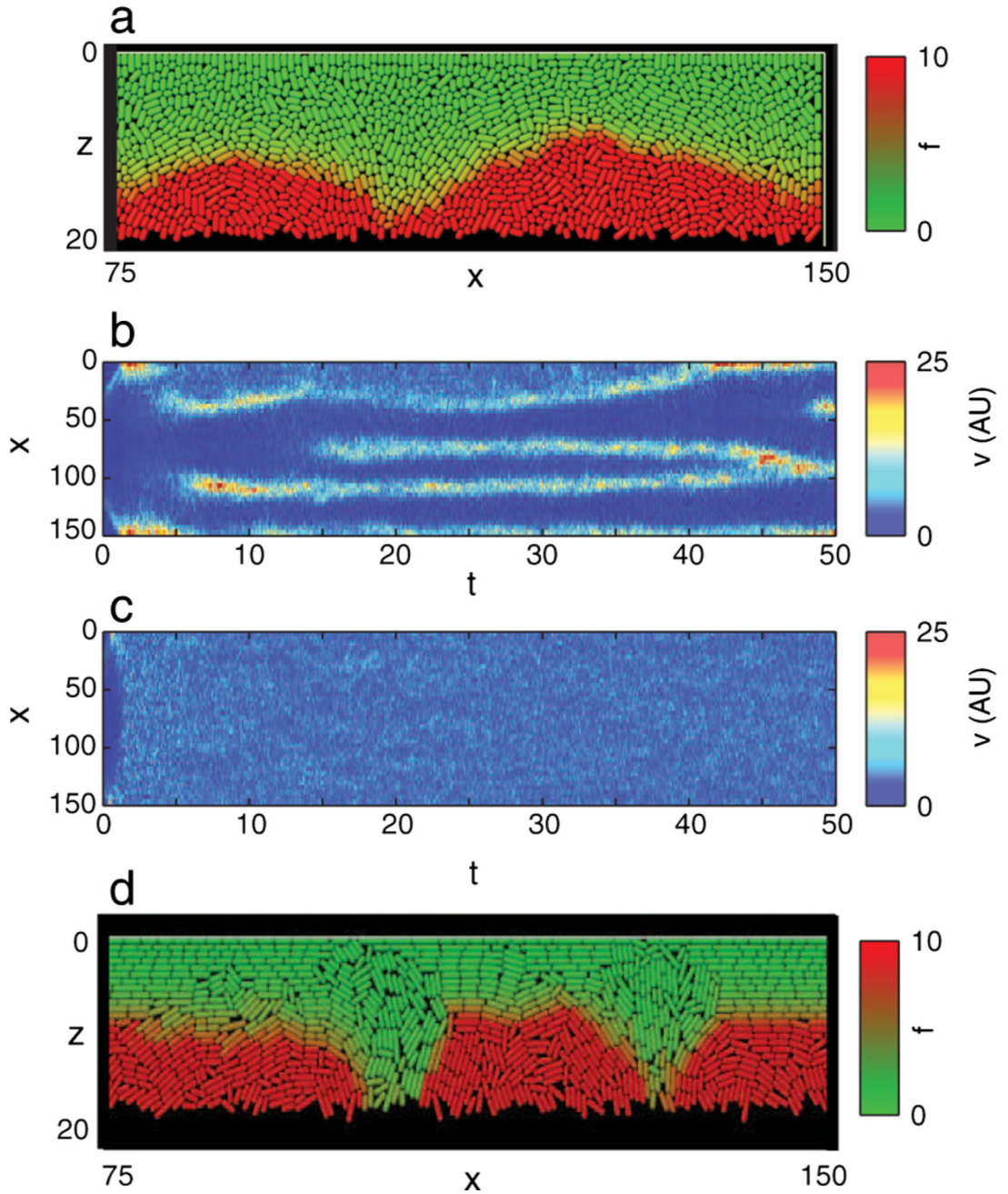
FIG. 3.
(color online). Streaming patterns in a wide side trap: (a) A snapshot of a cell population from a typical DES simulation of short rods ($\ell_{\text{div}}=3$) at time $t = 30$ of the simulation shown in panel (b). Cells are colored according to their values of f. Panels (b) and (c) show (x, t) diagrams of the z component of cell velocity averaged over the z axis. Both simulations had the same parameters and were initiated at $t = -15$) with a single cell, but for the simulation but in (b) f was allowed to evolve freely from the very beginning while in (c) f was fixed at $c(z)/2$ until time $t = 5$ and then relaxed. (d) Snapshot of the population of longer rods ($\ell_{\text{div}}=5$). Parameters are $L_x = 150$, $L_z = 20$, $\alpha = 0.5$, $\gamma = 0.5$, $c(z) = 1 + 200(z/L_z)^4$.